Nanotechnology Science and Technology

Organic Solvent-Free Synthesis of Magnetic Nanocrystals with Controlled Particle Sizes

Tomohiro Iwasaki

Novinka

NANOTECHNOLOGY SCIENCE AND TECHNOLOGY

ORGANIC SOLVENT-FREE SYNTHESIS OF MAGNETIC NANOCRYSTALS WITH CONTROLLED PARTICLE SIZES

TOMOHIRO IWASAKI

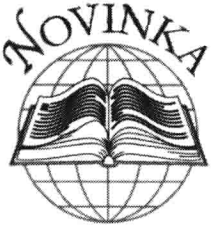

Nova Science Publishers, Inc.
New York

LIBRARY OF CONGRESS CATALOGING-IN-PUBLICATION DATA

Iwasaki, Tomohiro.
Organic solvent-free synthesis of magnetic nanocrystals with controlled particle sizes / Tomohiro Iwasaki.
p. cm.
Includes index.
ISBN 978-1-61122-500-6 (softcover)
1. Nanocrystals. 2. Magnetite crystals. I. Title. TA418.9.N35I985 2010
548--dc22 2010038648

Published by Nova Science Publishers, Inc. † New York

NANOTECHNOLOGY SCIENCE AND TECHNOLOGY

ORGANIC SOLVENT-FREE SYNTHESIS OF MAGNETIC NANOCRYSTALS WITH CONTROLLED PARTICLE SIZES

NANOTECHNOLOGY SCIENCE AND TECHNOLOGY

Additional books in this series can be found on Nova's website under the Series tab.

PREFACE

Magnetite (Fe_3O_4), which is an important member of spinel type ferrites, has been widely used in various industrial products such as recording materials because it has the excellent magnetic properties. Recently, bio-applications of Fe_3O_4 nanocrystals, e.g., magnetic resonance imaging, drug delivery, and hyperthermia, have attracted much attention because of the non-toxicity property and high chemical stability. Thus, the demand for Fe_3O_4 is increasing, and industrial synthesis methods which can meet the demand are needed. The synthesis processes should have the low environmental impact and must prepare the Fe_3O_4 nanocrystals with precisely controlled particle sizes suitable for the applications because the magnetic properties depend strongly on the particle size. Therefore, we have synthesized the size-controlled Fe_3O_4 nanocrystals using organic solvent-free conventional and novel methods: hydrothermal and mechanochemical synthesis methods. In the hydrothermal synthesis, ferrous and ferric hydroxides are coprecipitated or sequentially formed in high alkaline solutions, and then the suspension thus obtained is heated under a hydrothermal condition. In the coprecipitation operation, the molar ratio of ferrous ion to ferric ion is varied. Furthermore, the anionic species existing together with the iron ions are controlled. This synthesis method could control the particle size between 10 and 40 nm. On the other hand, we have developed a novel synthesis method using mechanochemical effect in order to prepare Fe_3O_4 nanocrystals with high crystallinity without using any environment-unfriendly additives such as toxic organic solvents and additional heating treatments. In this method, a tumbling ball mill is used as a synthesis reactor, and the suspension of ferrous and ferric hydroxides is ball-milled under a cooling condition. The solid phase reaction between ferrous and ferric hydroxides progresses owing to not the heat energy but the

mechanical energy. This method provides superparamagnetic Fe_3O_4 nanocrystals with a size of less than 10 nm.

NOMENCLATURE

a coefficient in Eq. (23) (s^{b-1})
b coefficient in Eq. (23) (–)
E impact energy of balls per unit time defined by Eq. (19) ($J \cdot s^{-1}$)
E_r impact energy of balls per single revolution of vessel defined by Eq. (20) (J)
$\boldsymbol{F}_n$ contact force acting on ball in normal direction (N)
$\boldsymbol{F}_t$ contact force acting on ball in tangential direction (N)
f average number of contact points per unit time (s^{-1})
$\boldsymbol{g}$ gravity acceleration ($m \cdot s^{-2}$)
I peak intensity at $2\theta = 21.2°$ of sample obtained by ball-milling (–)
I_b inertia moment of ball ($kg \cdot m^2$)
I_m peak intensity at $2\theta = 21.2°$ of sample before ball-milling (–)
k coefficient indicating reaction rate constant (s^{-1})
k' coefficient indicating reaction rate constant (–)
M mass of ball (kg)
m initial molar ratio of ferrous lactate to total ferrous ion defined by Eq. (6) (–)
m' addition molar amount of sodium salt defined by Eq. (7) (–)
N rotational speed of vessel (s^{-1})
$\boldsymbol{n}$ unit vector in normal direction at contacting point (m)
n_t number of collisions with energy exceeding threshold value (s^{-1})
r radius of ball (m)
$\boldsymbol{T}$ torque caused by tangential contact force (N·m)
t milling time (s)
$\boldsymbol{v}$ relative velocity of contacting ball ($m \cdot s^{-1}$)
$\boldsymbol{v}_n$ relative velocity of contacting ball in normal direction ($m \cdot s^{-1}$)
$\boldsymbol{v}_t$ relative velocity of contacting ball in tangential direction ($m \cdot s^{-1}$)

$\boldsymbol{X}$ position of ball (m)
x amount of magnetite in product (mol)
Y_b Young's modulus of ball (Pa)
Y_w Young's modulus of vessel (Pa)

GREEK LETTERS

α constant depending on restitution coefficient in Eq. (18) (–)
β initial molar ratio of ferrous ion to ferric ion (–)
γ content of magnetite in virtual product (%)
$\boldsymbol{\delta}$ overlap displacement between contacting balls (m)
$\boldsymbol{\delta}_n$ overlap displacement between contacting balls in normal direction (m)
$\boldsymbol{\delta}_t$ overlap displacement between contacting balls in tangential direction (m)
η_n damping coefficient in normal direction ($kg \cdot s^{-1}$)
η_t damping coefficient in tangential direction ($kg \cdot s^{-1}$)
κ_n stiffness in normal direction ($N \cdot m^{-3/2}$)
κ_t stiffness in tangential direction ($N \cdot m^{-1}$)
μ sliding friction coefficient (–)
ξ diffraction intensity ratio defined by Eq.(21) (–)
σ_b Poisson's ratio of ball (–)
σ_w Poisson's ratio of vessel (–)
$\boldsymbol{\omega}$ angular velocity of ball (s^{-1})

CONTENTS

Chapter 1

INTRODUCTION

Iron oxides powders have been used as color pigments for a long time, and the industrial uses, in particular, the applications to magnetic materials using magnetite (Fe_3O_4) and maghemite (γ-Fe_2O_3) such as recording media have rapidly expanded since the beginning of the 20th century because of the excellent magnetic properties (Buxbaum and Pfaff, 2005). At present, magnetic iron oxides are also utilized for printing and electrophotography such as copying toner (Ochiai *et al.*, 1994) and carrier powders (Hakata, 2002). Recently, the non-toxicity property and high chemical stability of Fe_3O_4 have attracted much attention, and many biomedical applications of Fe_3O_4 nanoparticles have been studied actively: e.g., sensors (Tanaka *et al.*, 2006; Erdem *et al.*, 2007; Hai *et al.*, 2008), magnetic resonance imaging (MRI) (Chouly *et al.*, 1996; Wan *et al.*, 2007; Hong *et al.*, 2008), drug delivery system (DDS) (Lin *et al.*, 2007; Zhang and Misra, 2007), and cancer therapy (Fukumori and Ichikawa, 2006; Wang *et al.*, 2007a; Murakami *et al.*, 2008).

In order that Fe_3O_4 nanoparticles exhibit required magnetic efficiency in biomedical applications, Fe_3O_4 nanoparticles should have the controlled size suitable for the applications because the magnetic properties depend strongly on the particle size. For example, Fe_3O_4 nanoparticles of about 10 to 20 nm are used for DDS and cancer therapy, and below 10 nm of superparamagnetic Fe_3O_4 nanoparticles with good dispersibility are needed for MRI. For preparing the size-controlled Fe_3O_4 nanoparticles, various synthesis methods using solid, liquid and gaseous phases reactions have been developed: e.g., thermal decomposition of iron complex in organic solvent (Park *et al.*, 2004), pulsed laser ablation (PLA) (Paramês *et al.*, 2007), mechanochemical processing (Qian *et al.*, 1994), and micro-emulsion (Zhou

et al., 2001; Gotić *et al.*, 2007). Many synthesis methods developed to control the particle size so far have serious problems that the synthesis process is relatively complicated and organic solvents which are unsuitable for biomedical applications are often used.

Among the preparation methods, coprecipitation of ferrous and ferric hydroxides in organic solvent-free water system is useful because of its simplicity of the process and relatively low environmental impact (Visalakshi *et al.*, 1993; Wen *et al.*, 2008; Valenzuela *et al.*, 2009; Zhao *et al.*, 2009; Iwasaki *et al.*, 2010a; Iwasaki *et al.*, 2010b). However, this method has a disadvantage that obtained Fe_3O_4 nanoparticles tend to have relatively low crystallinity and poor magnetic properties (Martínez-Mera *et al.*, 2007; Wu *et al.*, 2007; Wu *et al.*, 2008). Therefore, following hydrothermal treatment of the suspension of precursor, ferrous hydroxide-goethite composites, formed by the coprecipitation is effective to improve easily the crystallinity (Qian *et al.*, 1994). During the hydrothermal treatment, the Fe_3O_4 nanoparticles have a tendency to aggregate by heating. Thus, surfactant is often added to the suspension for preventing the aggregation (Shokuhfar *et al.*, 2008; Wang *et al.*, 2007b). For medical applications, however, it is undesirable to use any surfactants because surfactants are unsuitable for human body, and if used, sufficient separation and washing treatments to remove surfactants are needed, leading to a complicated preparation process. Accordingly, a preparation method without using any surfactants is required in the hydrothermal synthesis of Fe_3O_4 nanoparticles.

This text provides several hydrothermal synthesis methods we developed to control the size of Fe_3O_4 nanoparticles without using any surfactants. In addition, we propose a novel preparation process in which formation and crystallization of Fe_3O_4 nanoparticles are promoted by means of not heat energy but mechanical energy.

Chapter 2

SIZE CONTROL IN HYDROTHERMAL SYNTHESIS

EFFECT OF FERROUS/FERRIC IONS MOLAR RATIO ON REACTION MECHANISM FOR HYDROTHERMAL SYNTHESIS OF MAGNETITE NANOPARTICLES

The reaction mechanism in the hydrothermal synthesis of Fe_3O_4 is as follows. When an alkaline solution is added to an acidic solution containing ferric and ferrous ions, ferrous hydroxide ($Fe(OH)_2$) and goethite (α-FeOOH) which is transformed from ferric hydroxide ($Fe(OH)_3$) are coprecipitated according to Eqs. (1) to (3).

$$Fe^{2+} + 2OH^- \rightarrow Fe(OH)_2 \quad (1)$$

$$Fe^{3+} + 3OH^- \rightarrow Fe(OH)_3 \quad (2)$$

$$Fe(OH)_3 \rightarrow \alpha\text{-}FeOOH + H_2O \quad (3)$$

At the coprecipitation, $Fe(OH)_2$ grows on α-FeOOH, resulting in formation of the $Fe(OH)_2$-α-FeOOH composites. And then, a part of them is converted into homogeneous Fe_3O_4 according to the following solid phase reaction (Lian *et al.*, 2004).

$$Fe(OH)_2 + 2\alpha\text{-}FeOOH \rightarrow Fe_3O_4 + 2H_2O \quad (4)$$

The reaction rate changes remarkably depending on the molar ratio of Fe^{2+}/Fe^{3+} (Fan *et al.*, 2001) and the presence of oxidizing (Iida *et al.*, 2007) and reducing agents (Wang *et al.*, 2004). Accordingly, for the formation of Fe_3O_4 nanoparticles with controlled sizes, the initial Fe^{2+}/Fe^{3+} molar ratio of 0.5 corresponding to the stoichiometric ratio in the Fe_3O_4 formation reaction is needed and no use of oxidizing and reducing agents is preferred. It is well known that this reaction is relatively slow at room temperature and that the reaction rate can be increased by heating. Therefore, effects of the Fe^{2+}/Fe^{3+} molar ratio on the reaction mechanism were examined.

All chemicals used in the experiments were of analytical reagent grade and were used without further purification. A proper amount of ferrous sulfate heptahydrate ($FeSO_4 \cdot 7H_2O$) and ferric chloride hexahydrate ($FeCl_3 \cdot 6H_2O$) were dissolved in 40 ml of deionized and deoxygenated water in a stainless steel autoclave. After several minutes, 20 ml of 1.0 kmol/m^3 sodium hydroxide (NaOH) solution was added into the solution at a constant addition rate under vigorous stirring using a magnetic stirrer in an argon atmosphere for oxidation prevent of Fe^{2+}. The addition rate of NaOH solution was set to be 3.0 ml/min for forming the precipitates homogeneously.

The initial Fe^{2+}/Fe^{3+} molar ratio β in the solution was varied in the range of β = 0.25 to 2.0 by adjusting the amount of $FeSO_4$ under the constant amount of $FeCl_3$ (= 2 mmol). After air in the autoclave was replaced with argon, the sealed autoclave was maintained at 120°C for a given heating time in an electric oven and then cooled down to room temperature. The heating time was varied as 0 (i.e., without heating), 4 and 20 h. The obtained black precipitate was washed with deionized water and decanted after centrifugation at the centrifugal acceleration of 1500 G. After the washing operation was repeated 3 times, the sample was dried overnight in air at 80°C.

The powder X-ray diffraction (XRD) pattern of samples was measured with CuKα radiation ranging from 2θ = 10 to 80° at a scanning rate of 1.0°/min using a Rigaku RINT-1500 powder X-ray diffractometer. Figure 1 shows the XRD patterns of samples obtained after heating for a given time under various β. The morphology of prepared samples was observed with a field emission scanning electron microscope (FE-SEM, JEOL JSM-6700F). Figures 2 and 3 indicate the SEM images of samples prepared under representative molar ratios of β = 0.5 and 2.0 as an example, respectively. In addition, the average crystallite size was calculated from the full-width at half-maximum (FWHM) of the Fe_3O_4 (311) diffraction peak at $2\theta \approx 35.5°$ using the Scherrer's formula. Figure 4 shows the change in the average

crystallite size with the heating time. As can be seen in these figures, in the samples prepared at $\beta \leq 0.5$ without heating, the typical peak of α-FeOOH phase was seen at $2\theta \approx 21.2°$ in the XRD patterns, and the needle-shaped particles corresponding to α-FeOOH were observed (see Figure 2a) because of incomplete reaction. At $\beta = 0.5$, α-FeOOH was consumed as the reaction progressed by heating and then homogeneous Fe_3O_4 phase with a relatively high crystallinity could be obtained. However, when $\beta = 0.25$, α-FeOOH still remained after heating for 20 h because of the lack of $Fe(OH)_2$. No peaks were observed in the XRD patterns at $2\theta = 14.9$, 23.7 and 26.0°, which are typical peaks of maghemite (γ-Fe_2O_3) corresponding to (103) and (110) lines, (106) and (203) lines, and (213) and (116) lines, respectively. In addition, the lattice constant calculated from the XRD patterns of the samples of $\beta = 0.5$ to 2.0 after heating for 20 h was between 8.37 and 8.42 Å, and close to that of Fe_3O_4 (8.396 Å) compared to that of γ-Fe_2O_3 (8.345 Å). These also support that the samples of $\beta \geq 0.5$ after heating were Fe_3O_4 phase.

As can be seen in Figure 2, at $\beta = 0.5$ the particle size after heating for 20 h was almost the same (about 30 nm) as that before heating whereas the average crystallite size increased with increasing in the heating time as shown in Figure 4. This implies that the reaction progresses rapidly by heating and the crystal nucleation (i.e., formation of precursors) of Fe_3O_4 mainly occurs, resulting in inhibition of the crystal growth, and that the coalescence of crystallites in the inside of a particle increases the crystallinity.

On the other hand, when $\beta \geq 1.0$ in which the amount of $Fe(OH)_2$ in the starting solution exceeded the stoichiometric ratio, α-FeOOH was consumed almost completely before heating as shown in Figures 1a and 3a. Also, as can be seen in Figures 2 and 3a, the particle size before heating was almost the same as that at $\beta = 0.5$. The results reveal that the reaction rate increases even at room temperature in the presence of surplus $Fe(OH)_2$. In the heating period, the average crystallite size increased as the heating time elapsed similar to the case of $\beta = 0.5$. However, the particle size and crystallinity increased greatly with increasing in the heating time. This tendency was remarkable as β increased, and especially at higher β for longer heating times, the nanoparticles with a shape close to a regular octahedron, which is the crystal form of Fe_3O_4 (Yu *et al.*, 2006), were obtained. The results suggest that the crystallization of Fe_3O_4 nanoparticles progresses in the heating period according to the different mechanisms depending on the initial $Fe(OH)_2$ content; the growth of crystallites remarkably occurs at higher β in the heating period, caused by the Schikorr reaction in which

$Fe(OH)_2$ is transformed into Fe_3O_4 at higher temperatures according to the following reaction (Schikorr, 1929; Shipko and Douglas, 1956).

$$3Fe(OH)_2 \rightarrow Fe_3O_4 + H_2 + 2H_2O \quad (5)$$

The rate of the Schikorr reaction is very slow as compared with that of the reaction expressed by Eq. (4). Therefore, in the presence of excess $Fe(OH)_2$ the crystal nucleation was completed rapidly at room temperature according to Eq. (4), and then using surplus $Fe(OH)_2$ the crystallites in the Fe_3O_4 nanoparticles grew up slowly under hydrothermal conditions according to Eq. (5) rather than their coalescence.

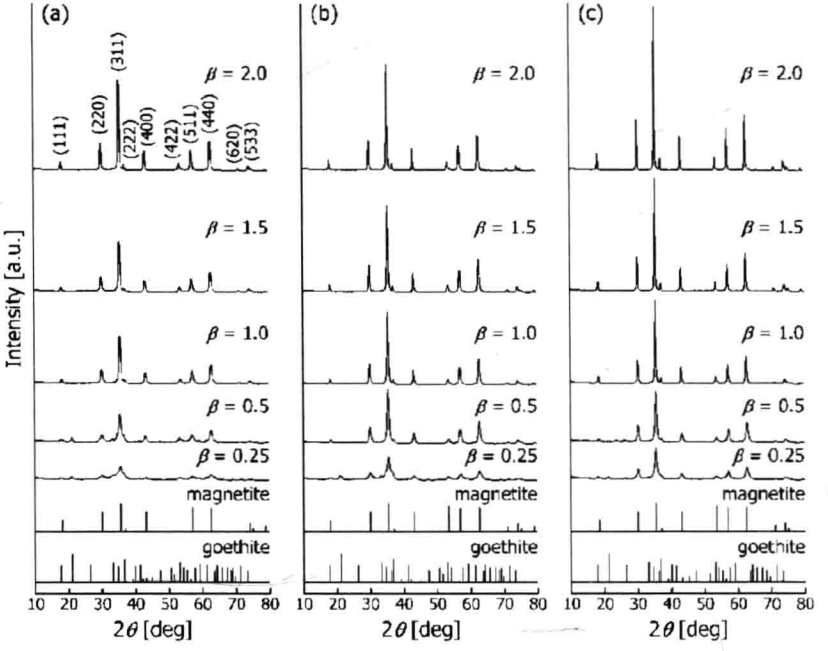

Figure 1. XRD patterns of samples prepared under various Fe^{2+}/Fe^{3+} molar ratios β (a) before and after heating for (b) 4 h and (c) 20 h. Solid bars indicate the standard patterns for magnetite (ASTM card #11-614) and goethite (ASTM card #3-249).

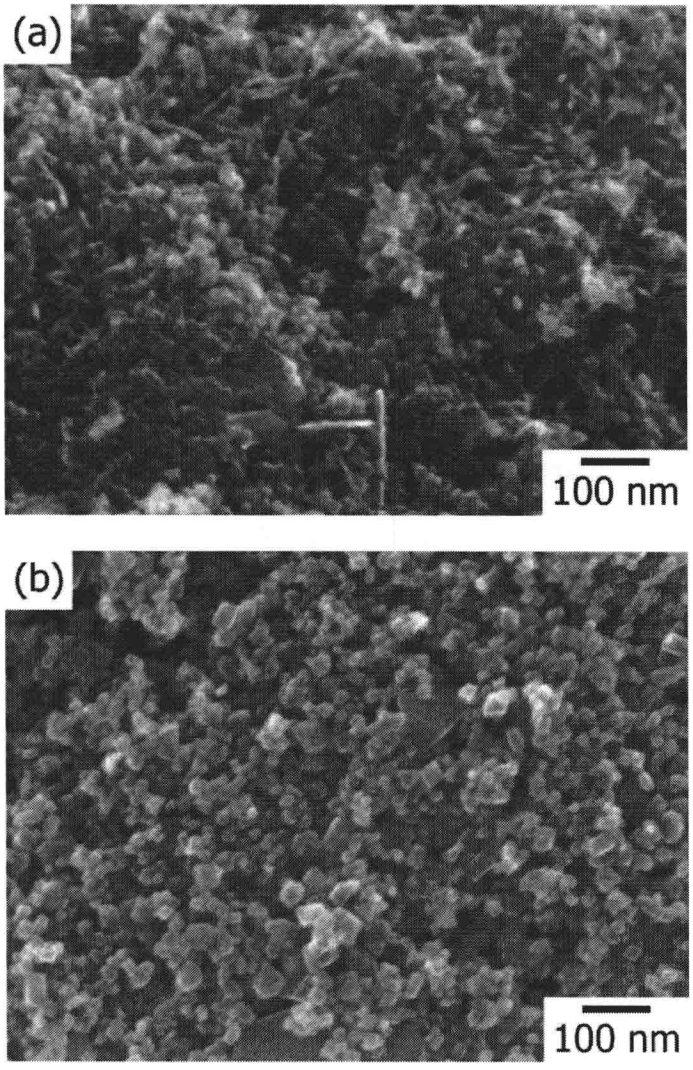

Figure 2. SEM images of samples obtained (a) before and (b) after heating for 20 h at $\beta = 0.5$.